Alterations to the Primer Grip of p66 HIV-1 Reverse Transcriptase and Their Consequences for Template-Primer Utilization†

Madhumita Ghosh,‡ Pamela S. Jacques,‡ David W. Rodgers,§ Michele Ottman,|| Jean-Luc Darlix,|| and Stuart F. J. Le Grice*,‡

Center for AIDS Research and Division of Infectious Diseases, Case Western Reserve University School of Medicine, 10900 Euclid Avenue, Cleveland, Ohio 44106, Department of Molecular and Cellular Biology, Harvard University, Cambridge, Massachusetts 02138, and Labo Retro, Ecole Normale Superieure de Lyon, 46, Allee de'Italie, Lyon, France

Received November 22, 1995; Revised Manuscript Received March 20, 1996⊗

ABSTRACT: Alanine scanning mutagenesis was undertaken to evaluate the structural significance of Met^{230}−His^{235} of the 66 kDa subunit of p66/p51 human immunodeficiency virus reverse transcriptase (HIV-1 RT). Together with Glu^{224}−Trp^{229}, these residues provide the framework of the p66 "primer grip", whose proposed role is maintaining the primer terminus in an orientation appropriate for nucleophilic attack on an incoming dNTP. Of these residues, altering Leu^{234} results in a p66 subunit incapable of associating into heterodimer. The remaining selectively mutated enzymes were successfully reconstituted and purified to homogeneity for evaluation of RT-associated activities. We show here that alterations to any residue within the p66 -Trp^{229}-Met^{230}-Gly^{231}-Tyr^{232}-quartet alter functions associated with both the DNA polymerase and ribonuclease H (RNase H) domains. Detailed analysis of mutant p66^{Y232A}/p51 with an intact or a model "precleaved" RNA−DNA hybrid suggests an altered RNase H phenotype could result from relocation of template-primer in the nucleic acid binding cleft. As a consequence, template nucleotide −8 is positioned in the immediate vicinity of the RNase H catalytic center rather than nucleotide −17.

The availability of high-resolution three-dimensional structures for unliganded (Rodgers et al., 1995), DNA-bound (Jacobo-Molina et al., 1993), and nevirapine-containing human immunodeficiency virus type 1 reverse transcriptase (HIV-1 RT)[1] (Kohlstaedt et al., 1992; Smerdon et al., 1994) permits a precise analysis of how individual subdomains and subunits contribute to the multiple activities of this highly versatile enzyme. For example, the observation that the p51 connection subdomain lies between its palm and thumb to obscure its DNA polymerase active site (Kohlstaedt et al., 1992) explains the inactivity previously documented for this heterodimer-associated subunit (Le Grice et al., 1991). Despite the inactivity of p51, analysis of the site of action for nonnucleoside drugs (Nanni et al., 1993) implicated residues of this subunit in binding the inhibitor TSAO-T, a notion later verified experimentally by Jonckheere et al. (1994). More recently, information on the p66−p51 subunit interface has promoted the design of short peptides which inhibit dimerization of the HIV-1 enzyme (Divita et al., 1994). These studies illustrate the necessity of complementary structural and biochemical approaches when studying HIV RT, which collectively should accelerate efforts to design novel and more potent antiviral drugs to reduce the rate of HIV infection and spread of acquired immunodeficiency syndrome (AIDS).

Using a combination of subunit-selective mutagenesis and *in vitro* reconstitution (Le Grice et al., 1991), we recently reported the consequence of amino acid substitutions between Glu^{224} and Trp^{229} of the heterodimer-associated p66 subunit (Jacques et al., 1994a). This region includes the β11b−β12 connecting loop (Lys^{223}−Pro^{226}, adopting the nomenclature of Jacobo-Molina et al., 1993) and β-strand 12 (Phe^{227}−Trp^{229}), shown by Xiong and Eichbusch (1990) to be conserved among several retroviruses and later proposed to constitute a component of the "primer grip" (Nanni et al., 1993). In the RT-DNA cocrystal (Jacobo-Molina et al., 1993) the β12−β13 hairpin (p66 residues Phe^{227}−His^{235}, Figure 1) maintains the primer terminus in the appropriate orientation for nucleophilic attack on an incoming dNTP. Although we noted little difference when Phe^{227} and Leu^{228} were altered, replacement of Trp^{229} substantially reduced the affinity of recombinant RT for template-primer *in vitro* and loss of viral infectivity *in vivo* (Jacques et al., 1994a). At the same time, a contribution of Phe^{227} and Trp^{229} toward the architecture of the nonnucleoside inhibitor binding pocket was proposed by Smerdon et al. (1994). Involvement of the β12−β13 hairpin in multiple functions of HIV-1 RT therefore makes an important case for a detailed molecular and biochemical analysis of the complete motif, since it remains to be established whether all residues or only a subset control primer grip function. Figure 1 illustrates that β-strands 12−15 constitute a β-sheet at the base of the p66 thumb subdomain, which is implicated in binding the nucleic acid duplex and translocation (Nanni et al., 1993). Therefore, alterations to the primer grip could conceivably perturb the geometry of this β-sheet, influencing how duplex nucleic

† Supported by NIH Grants GM 52263 (to S.F.J.L.G.) and GM 39589 (D.W.R.). M.G. and P.S.J. contributed equally to data presented in this paper.

* Corresponding author: Tel (216) 368-6989; Fax (216) 368-2034; e-mail sfl@po.cwru.edu.

‡ Case Western Reserve University School of Medicine.

§ Harvard University.

|| Ecole Normale Superieure de Lyon.

⊗ Abstract published in *Advance ACS Abstracts,* June 15, 1996.

[1] Abbreviations: DNase I, deoxyribonuclease I; HIV, human immunodeficiency virus; nt, nucleotides; PBS, primer binding site; RT, reverse transcriptase; RNase H, ribonuclease H.

S0006-2960(95)02773-5 CCC: $12.00

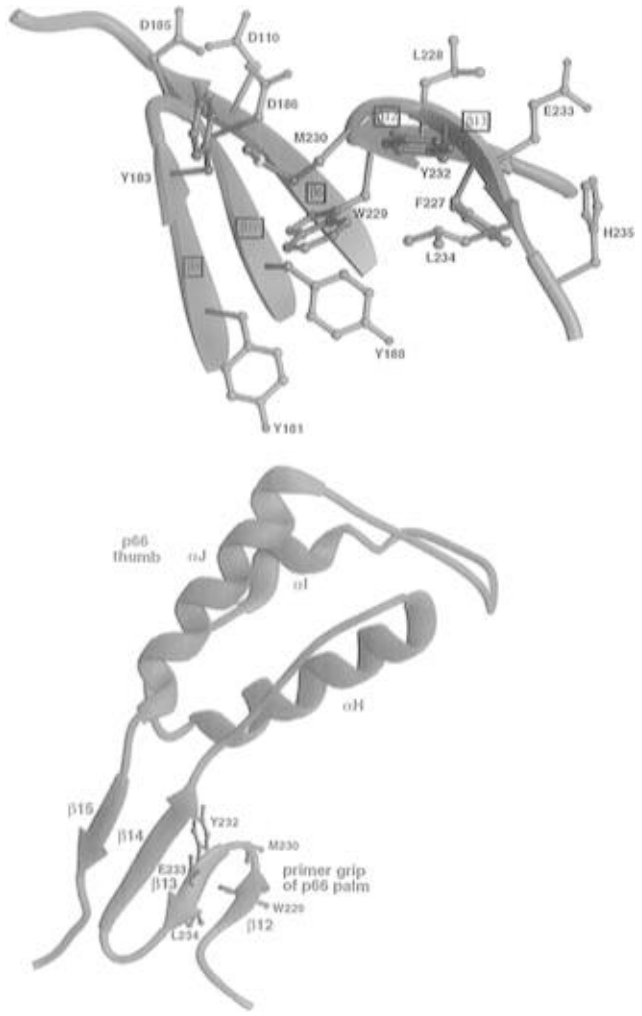

FIGURE 1: (Upper) Disposition of the side chains of Phe^{227}−His^{235} within structural elements comprising the β12−β13 hairpin, or primer grip, of heterodimer-associated p66. In addition to the primer grip, secondary structural elements from the DNA polymerase catalytic center and relevant side-chain atoms have been highlighted. (Lower) Spatial relationship of the p66 primer grip motif to its thumb subdomain. The thumb designation, i.e., residues 244 and 322, is according to Jacobo Molina et al. (1993). The β12−β13 hairpin of the p66 palm is colored red, while α-helices and β-strands of the thumb are colored green. A β-sheet at the base of the thumb is comprised of β-strands 12−15.

acid is accommodated during both RNA- and DNA-dependent DNA synthesis.

In this paper, we evaluated the consequences of amino acid substitutions in the β12−β13 connecting loop (Met^{230} and Gly^{231}) and β-strand 13 (Tyr^{232}−His^{235}) of p66 HIV-1 RT. Mutant p66 polypeptides were reconstituted into a heterodimer with a wild-type p51 subunit, after which the DNA polymerase and RNase H activities of the selectively mutated enzymes were determined. Our data suggest substitutions within the β12−β13 connecting loop (Met^{230} and Gly^{231}) and flanking residues (Trp^{229} and Tyr^{232}) manifest themselves in alterations at both catalytic centers. A detailed analysis of the RNase H activity of mutant p66^{Y232A}/p51 was undertaken with intact and "precleaved" RNA−DNA hybrids, the latter of which represents a −17 hydrolysis intermediate. Our findings suggest the altered RNase H phenotype of this mutant could reflect a preference for its polymerization-independent mode of RNase H activity (Peliska & Benkovic, 1992), i.e., cleavage of the template at nucleotide −8. A complementary *in vivo* analysis, where the mutation is present in each subunit, supports the results of our *in vitro* investigations.

EXPERIMENTAL PROCEDURES

Construction and Purification of Selectively Deleted p66/p51 Mutants. *Bcg*I cassette mutagenesis was used to introduce alanine substitutions between Met^{230} and His^{235} of the 66 kDa RT gene of plasmid pRT (Jacques et al., 1994a). Mutant polypeptides were reconstituted into a heterodimer with wild-type p51, yielding the selectively mutated heterodimer series p66^{M230A}/p51−p66^{H235A}/p51. Reconstituted heterodimers were purified to homogeneity by metal chelate (Ni^{2+}−nitrilotriacetic acid−Sepharose) and ion-exchange chromatography (S-Sepharose) and stored in a 50% glycerol-containing buffer at −20 °C (Le Grice et al., 1995). Enzyme thus stored remained stable for several months.

DNA-Dependent DNA Polymerase Activity. DNA-dependent DNA polymerase activity was determined with a heteropolymeric 71-nt template to which a 36-nt, 5′ end-labeled primer was hybridized (Figure 3A; Wöhrl et al., 1995a). Template and primer were annealed at a 2:1 ratio by heating to 85 °C in a buffer of 10 mM Tris-HCl, pH 7.5, 25 mM NaCl, and 0.2 mM $MgCl_2$, followed by cooling to room temperature over 2 h. RT (0.6 pmol) was incubated with 0.6 pmol of template-primer at 37 °C in a buffer containing 50 mM Tris-HCl, pH 8.0, 10 mM $MgCl_2$, 80 mM NaCl, 5 mM DTT, and 50 μM each of dATP, dTTP, dCTP, and dGTP and a final reaction volume of 60 μL. Aliquots were removed for analysis between 5 s and 10 min after DNA synthesis was initiated; products were fractionated by high-resolution denaturing gel electrophoresis through 10% polyacrylamide gels, followed by autoradiographic visualization.

Oligoribonucleotide-Primed (−) Strong-Stop DNA Synthesis. A PBS-containing RNA template, flanked by unique 5′ (U5) and repeat (R) sequences of the HIV-1_{HXB2} genome (Ratner et al., 1986), was prepared from *Acc*I-cleaved pHIV-PBS by *in vitro* transcription (Arts et al., 1996). The primer was a 5′ end-labeled oligoribonucleotide complementary to the primer binding site of the viral genome (i.e., 18 nt). Template and primer were mixed at a 1:1 ratio in annealing buffer (10 mM Tris-HCl, pH 7.5, 25 mM KCl), heated to 85 °C, and then slowly cooled to allow formation of secondary structures. Template-primer (1.2 pmol) was preincubated with wild-type or mutant RT (2.4 pmol) in a buffer of 10 mM Tris-HCl, pH 7.5, 10 mM $MgCl_2$, 50 mM KCl, and 5 mM DTT prior to addition of dNTPs to 200 μM. The final reaction volume was 40 μL. DNA synthesis was allowed to proceed for 60 min at 37 °C, during which time products were sampled at intervals indicated in the text. Following high-voltage electrophoresis through denaturing 6% polyacrylamide gels, synthesis products were visualized by autoradiography.

RNase H Activity. For visualization of RNase H hydrolysis products, a 90-nt RNA template was radiolabeled at its 5′ terminus and hybridized to a 36-nt DNA primer as described previously (Jacques et al., 1994; Ghosh et al., 1995). Activity was determined in the absence of DNA synthesis. Radiolabeled hybrid was incubated with varying amounts of purified enzyme, in the absence of deoxynucleoside triphosphates, in a buffer of 50 mM Tris-HCl, pH 8.0,

80 mM NaCl, and 5 mM DTT. Hydrolysis was initiated by addition of $MgCl_2$ to a final concentration of 6 mM. Sample times were chosen to allow partial (5 s) and complete template hydrolysis (10 min), thereby permitting visualization of all hydrolysis. In addition to an autoradiographic analysis following high-resolution gel electrophoresis, quantitation was provided by phosphorimaging (Molecular Dynamics). Data analysis was accomplished using ImageQuant software provided by the supplier.

Two-Step RNase H Assays. In order to prepare a model RNA−DNA hybrid whose template was cleaved specifically at position −17, the substrate of the previous section was incubated for 30 min with the selectively deleted RT mutant described recently by Ghosh et al. (1995). Under these conditions, mutant enzyme locates itself over the primer 3′-OH to cleave endonucleolytically at template nucleotide −17 but fails to cleave further toward template nucleotide −8. The reaction mixture was then supplemented with an aliquot of wild type or mutant. In the second round of RNase H analysis, enzymes under evaluation were added either in stoichiometric amounts to mutant p66Δ8/p51 or at a 4-fold excess.

Infectivity of HIV-1 Containing Primer Grip Mutations. Mutations between Trp^{229} and His^{235} were introduced into the RT gene of the infectious proviral clone pNL4.3 (Adachi et al., 1986) as described by Jacques et al. (1994a). Proviral transfection of Cos 7 cells was performed by standard calcium precipitation (Chen & Okayama, 1987). Three days postinfection, supernatant from transfected cells was harvested and clarified by low-speed centrifugation (3000 rpm, 15 min). Virus p24 core antigen (CAp24) was determined by ELISA, while RT activity was determined by a modification of the protocol of Goff et al. (1981). The virus titer was assessed by infecting 1×10^6 human SupT1 cells (Smith et al., 1984) with 1 mL of clarified supernatant, or a 10-fold serial dilution, and virion-associated RT activity monitored between 4 and 20 days postinfection. For immunological analysis, virions were collected by ultracentrifugation through a 25% sucrose cushion in 25 mM Tris-HCl, pH 7.5, 50 mM NaCl, and 1 mM EDTA (TNE). Virion pellets were disrupted in TNE containing 1% SDS, after which total protein was fractionated by SDS−polyacrylamide gel electrophoresis. Following transfer to nitrocellulose membranes, CAp24 and p66/p51 RT were detected by chemiluminescence (Amersham).

RESULTS

Dimerization of Selectively Deleted Mutants. Although qualitative, metal chelate chromatography (Hochuli et al., 1988) provides a valuable first approximation of whether mutations in one RT subunit can alter the environment at the p66−p51 dimer interface. By attaching a polyhistidine extension selectively to the N-terminus of p51 RT, only p51-associated p66 is retained on the matrix. Through this approach, loss of enzyme activity through a failure to dimerize can be eliminated. The utility of "selectively tagged" heterodimers was recently demonstrated in our laboratory by the inability of p51 RT lacking 25 C-terminal residues to associate into heterodimer with wild-type p66 (Jacques et al., 1994b).

Figure 2A illustrates the subunit stoichiometry and purity of mutants $p66^{M230A}$/p51−$p66^{H235A}$/p51 following metal

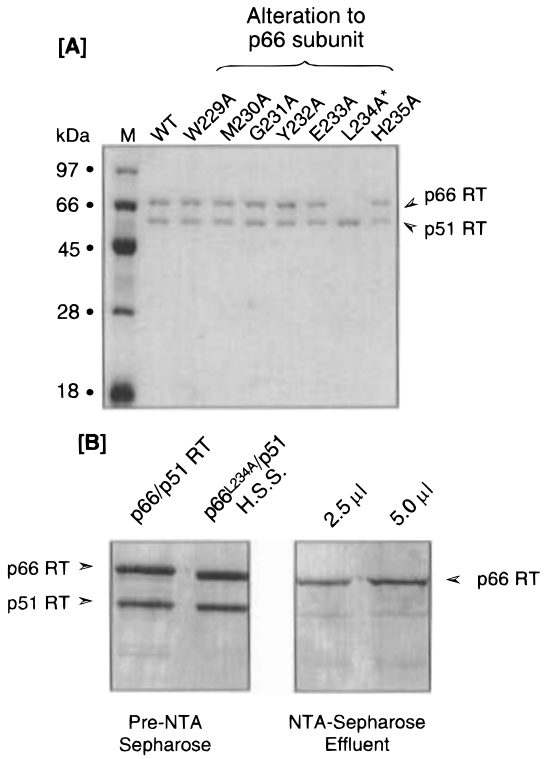

FIGURE 2: SDS−polyacrylamide gel electrophoresis of reconstituted heterodimers. [A] Analysis of enzymes mutated between Trp^{229} and His^{235} of their p66 subunit following a combination of metal chelate and ion-exchange chromatography. The alteration in heterodimer-associated p66 is indicated above each lane. M, protein molecular mass markers (in kDa). Migration positions of RT subunits are indicated. Proteins were visualized by Coomassie blue staining. [B] Immunological analysis of reconstitution between $p66^{L234A}$ and wild-type His-p51 RT. Left: proteins of the combined high-speed supernatants (HSS). Right: analysis of the Ni^{2+}−NTA−Sepharose effluent (i.e., nonbinding fraction). A polyclonal rabbit antiserum raised against purified p66/p51 RT was used for immunological detection.

chelate and ion-exchange chromatography. In contrast to our previous analysis of primer grip residues Glu^{224}−Trp^{229} (Jacques et al., 1994a), we found that substituting Leu^{234} with Ala yielded a p66 subunit unable to reconstitute into a heterodimer. This property was verified immunologically in the experiment of Figure 2B, where free $p66^{L234A}$ RT was detected in the NTA−Sepharose effluent, i.e., the nonbinding fraction. Coexpression of $p66^{L234A}$ RT with HIV-1 protease, a strategy which yields a doubly mutated heterodimer (Le Grice & Grüninger-Leitch, 1990), as well as reconstitution of $p66^{L234A}$ and His-$p51^{L234A}$ also failed to yield a heterodimer (K. J. Howard, unpublished observations). Although it is unclear why this alteration has such profound consequences, Smerdon et al. (1994) have reported that Leu^{234} in the nevirapine-binding pocket of p66 RT is never altered in nevirapine-resistant isolates, implicating its potential architectural role. In view of its inability to associate into heterodimer, enzyme altered at Leu^{234} was excluded from further *in vitro* analysis.

DNA-Dependent DNA Polymerase Activity. DNA-dependent DNA polymerase activity of mutants $p66^{W229A}$/p51−$p66^{H235A}$/p51 was evaluated on the heteropolymeric template-primer combination schematically illustrated in Figure 3A. Employing an equimolar enzyme−template-primer ratio and rapid sample analysis allowed us to follow the accumulation of early (P + 1−P + 4, where P defines the original 36-nt

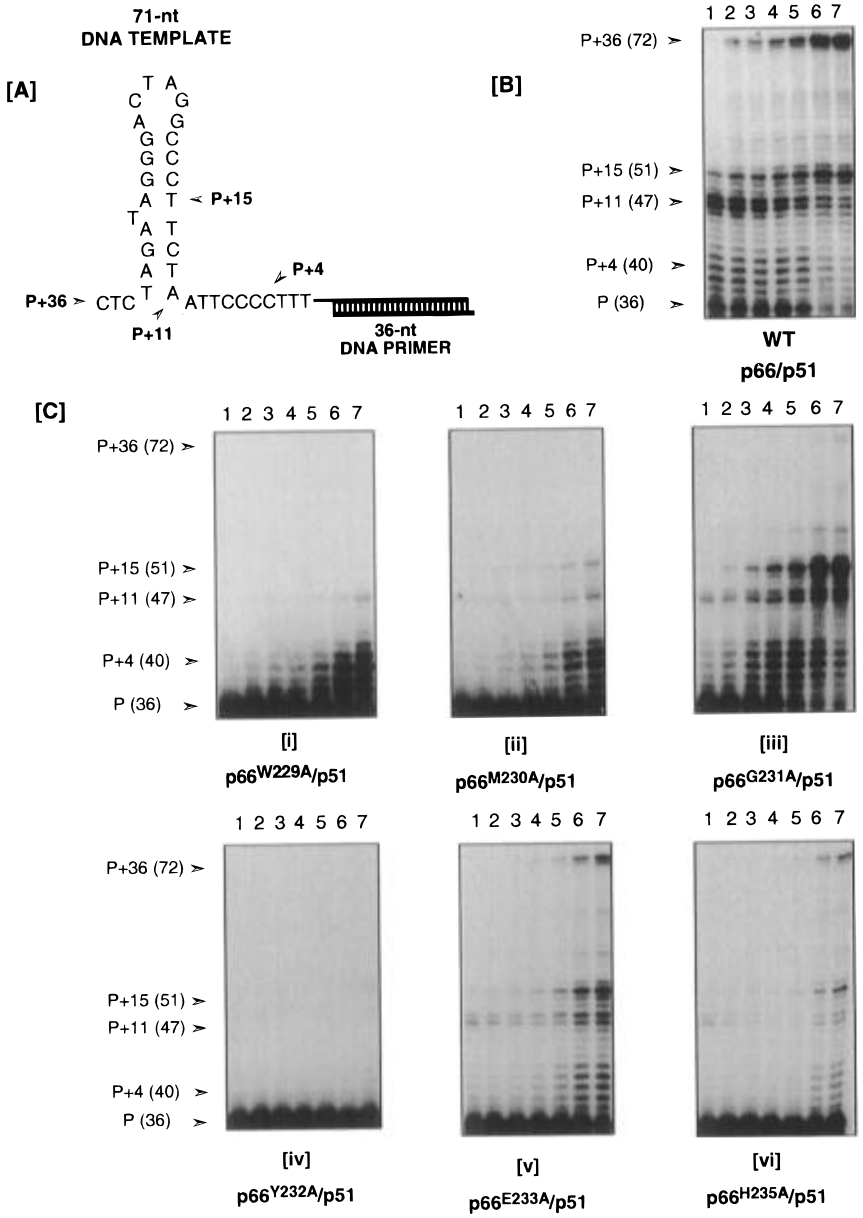

FIGURE 3: DNA-dependent DNA polymerase activities of primer grip mutants. [A] Schematic representation of the assay system, comprising a 71-nt template hybridized to a 5′ end-labeled 36-nt primer. The structure of the single-stranded template was determined by Wöhrl et al. (1995a). Notations P+4 etc. over the template refer to the number of nucleotides added to the primer, i.e., P+4 refers to a 40-nt DNA synthesis product. [B] Analysis of reconstituted, wild-type p66/p51 RT. A time course is presented where lane notations represent samples analyzed after 5 s (lane 1), 15 s (lane 2), 30 s (lane 3), 1 min (lane 4), 2 min (lane 5), 5 min (lane 6), and 10 min (lane 7). P, 36-nt DNA primer. [C] DNA-dependent DNA synthesis time course for selectively mutated primer grip mutants $p66^{W229A}$/p51 (panel [i]−$p66^{H235A}$/p51 (panel [vi]). Lane notations are as described in [B].

primer), stalled (P + 11−P + 15), and full-length (P + 36) cDNA synthesis products, which revealed substantial differences in several of the primer grip mutants.

For wild-type RT (Figure 3B), stalling at template nucleotides P + 11−P + 15 correlates with the ability to the translocating enzyme to disrupt a region of intramolecular base pairing (Figure 3A; Wöhrl et al., 1995a,b), after which there is virtually uninterrupted cDNA synthesis to the template 5′ terminus. Under the same conditions, the profiles most closely resembling the parental enzyme are those of $p66^{E233A}$/p51 and $p66^{H235A}$/p51 RT (Figure 3C, panels v and vi), although the overall level of synthesis was significantly reduced. Since wild-type RT was also reconstituted *in vitro*, differences in activity between this and mutants carrying substitutions at Glu^{233} and His^{235} are not attributable to trivial explanations such as the method of preparation. Of the remaining mutants, $p66^{G231A}$/p51 RT efficiently initiates DNA synthesis but stalls severely at the region of intramolecular base pairing defined by template nucleotides P + 11−P + 15 (panel iii). A third phenotype is defined by $p66^{W229A}$/p51 and $p66^{M230A}$/p51 RT, which support synthesis of short cDNA products (P + 1−P + 5), suggestive of a more distributive mode of DNA synthesis (panels i and ii). Finally, replacement of the p66 residue Tyr^{232} with Ala yields a mutant ($p66^{W232A}$/p51 RT) which supports little to no DNA synthesis (panel iv). Taken together, the data of Figure 3C suggest that primer grip architecture is most significantly altered by substitution of any residue within the -Trp^{229}-Met^{230}-Gly^{231}-Tyr^{232}- quartet. Perhaps most surprising was the observation that altering the highly conserved Gly^{231} of the $\beta12-\beta13$ connecting loop could be tolerated to a greater extent than any other member of the Trp^{229}−Tyr^{232} quartet.

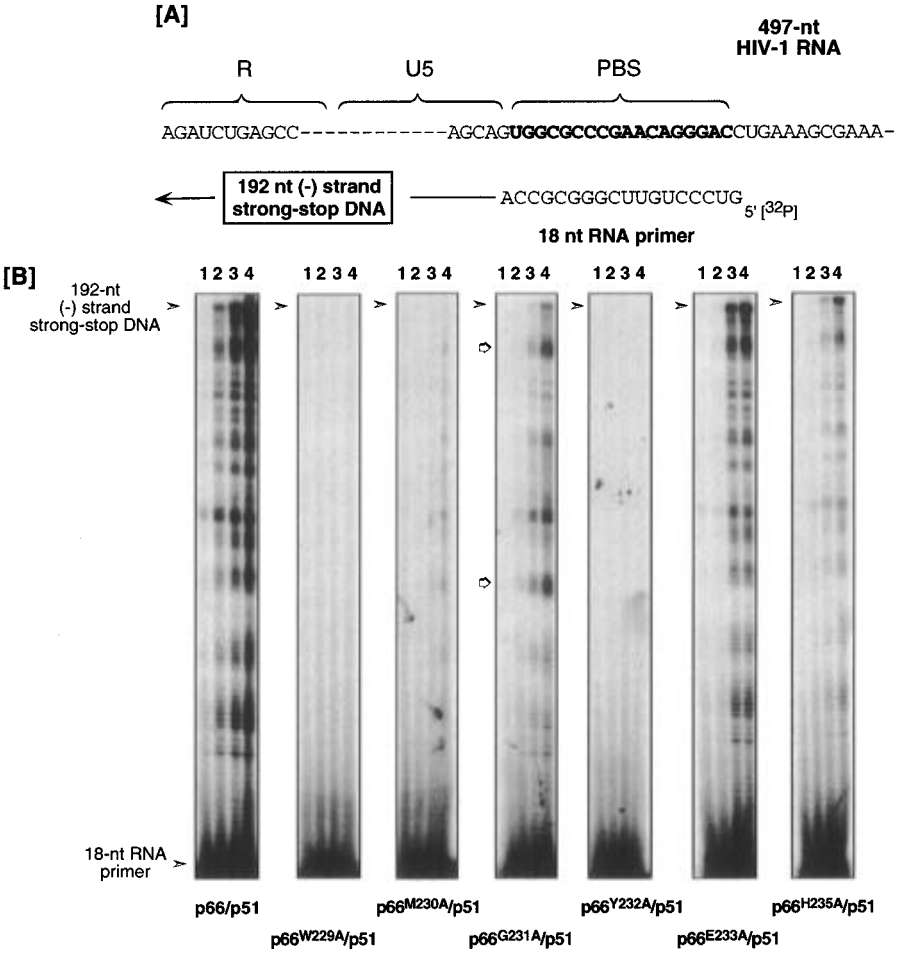

FIGURE 4: RNA-dependent DNA polymerase activities of primer grip mutants. [A] Schematic representation of the (−) strand strong-stop DNA synthesis system. The 497-nt RNA template generated by *in vitro* transcription contains R, U5, and PBS sequences of the HIV-1_{HXB2} genome. A 5′ end-labeled oligoribonucleotide (18 nt) hybridized to the PBS gives rise to a 192-nt (−) strand strong-stop DNA. [B] Ability of primer grip mutants to support RNA-primed (−) strand strong-stop DNA synthesis. The selectively mutated heterodimer is indicated under each panel, and a time course is presented for each enzyme. Samples were withdrawn for analysis after 5 min (lanes 1), 15 min (lanes 2), 30 min (lanes 3), and 60 min (lanes 4). The migration positions of the 192-nt strong-stop product and 18-nt RNA primer are indicated. The open arrow notation in reactions catalyzed by $p66^{G231A}$/p51 RT represents regions of enhanced stalling.

Supportive evidence for this finding was provided by DNase I footprinting, where a footprint was generated only with $p66^{G231A}$/p51 RT (data not shown). Furthermore, as will be demonstrated later, a $Gly^{231} \rightarrow Ala^{231}$ mutation was also tolerated *in vivo*, where it is present in each RT subunit.

RNA-Dependent DNA Polymerase Activity. In an attempt to provide a system more closely mimicking events during retroviral replication, RNA-dependent DNA polymerase activity was determined via the ability to support (−) strand strong-stop DNA synthesis from an oligoribonucleotide hybridized to the PBS of the viral RNA genome (Figure 4A; Arts et al., 1996). Under these conditions, Figure 4B indicates that wild-type RT extends the 18-nt primer into a 192-nt (−) strand strong-stop DNA product and is at the same time subject to pausing at several positions along the RNA genome. Under equivalent conditions, (−) strand synthesis is efficiently supported by $p66^{E233A}$/p51 RT and to a lesser extent by mutants $p66^{H235A}$/p51 and $p66^{G231A}$/p51. Despite reduced (−) strand synthesis, the position on the template at which pausing occurred with these mutants was unaffected, although the extent of pausing was slightly enhanced at certain positions with mutant $p66^{G231A}$/p51. This would be in keeping with the data of Figure 3, where $p66^{G231A}$/p51 RT efficiently initiated DNA-dependent DNA synthesis but stalls severely at a position on the template where intramolecular base pairing is adopted.

Although no full-length (−) strand strong-stop DNA is evident in a reaction catalyzed by $p66^{M230A}$/p51 RT, trace amounts of pause products could be detected after 60 min. Finally, mutants $p66^{W229A}$/p51 and $p66^{Y232A}$/p51 failed to support (−) strand strong-stop DNA synthesis, despite extending the incubation period for 60 min. The complete absence of DNA synthesis products in reactions catalyzed by enzymes mutated at Trp^{229} and Tyr^{232} of their p66 subunit suggests the defect lies at the stage of initiation rather than elongation.

Primer Grip Mutations Altering RNase H Activity. Although the primer grip is located on the palm subdomain of p66 RT, altering its geometry might influence template-primer positioning within the RNase H domain. RNase H activity was determined on a heteropolymeric 90-nt, 5′ end-labeled RNA hybridized at its 3′ terminus to a 36-nt DNA primer (Jacques et al., 1994a; Ghosh et al., 1995, Figure 5A). Although we previously followed loss of acid-precipitable counts from randomly generated RNA−DNA hybrids to evaluate RNase H activity (Schatz et al., 1989), recent data with HIV-1 RNase H mutants which support endonucleolytic cleavage at template nucleotide −17 but fail to process

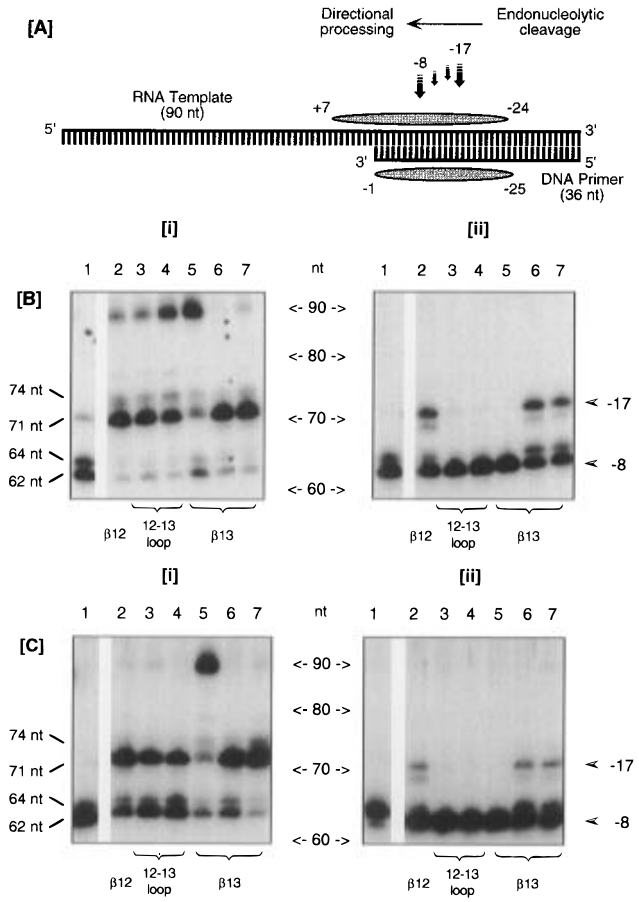

FIGURE 5: RNase H activities of primer grip mutants p66^{W229A}/p51−p66^{H235A}/p51. [A] Schematic representation of the heteropolymeric RNase H substrate, comprising a 5′ end-labeled 90-nt RNA template to which a 36-nt DNA primer is hybridized at the 3′ terminus (Ghosh et al., 1995). In the absence of DNA synthesis, template and primer nucleotides occupied by wild-type RT have been indicated (Wöhrl et al., 1995a). The positions at which cleavage produces the major −17 and −8 hydrolysis products are indicated. Arrows between these two positions represent positions of minor cleavage. [B] and [C] RNase H activity. Activity was determined at RT:RNA−DNA hybrid ratios of 2.5:1 ([B]) and 5:1 ([C]), in the absence of challenge, i.e., allowing multiple dissociation and rebinding events. In both cases, panel [i] illustrates the hydrolysis products following a 5 s incubation, while panel [ii] illustrates the products following incubation for 10 min. Lanes: 1, wild-type p66/p51; **2**, p66^{W229A}/p51; **3**, p66^{M230A}/p51; **4**, p66^{G231A}/p51; **5**, p66^{Y232A}/p51; **6**, p66^{E233A}/p51; **7**, p66^{H235A}/p51. The position of mutations within the β12−β13 hairpin is indicated under each panel.

further to template nucleotide −8 (Ghosh et al., 1995; Cirino et al., 1995) illustrate the importance of qualitatively assessing RNase H hydrolysis products (Le Grice, 1995). In the experiments of Figure 5B,C, RNase H activity was determined in the absence of DNA synthesis, and the hydrolysis products were evaluated after incubation times of 5 s and 10 min.

The hydrolysis profile from wild-type RT (Figure 5B, panels i and ii, lanes 1) supports the model predicted by enzyme binding template-primer with its DNA polymerase catalytic center located over the primer 3′ terminus (Peliska & Benkovic, 1992). The 71-nt hydrolysis product reflects endonucleolytic template cleavage 17 nt behind the primer terminus. With prolonged incubation (panel ii, lane 1), this is replaced by a 62-nt fragment, reflecting processing toward the 5′ terminus as far as template nucleotide −8. Most primer grip mutants display a similar pattern, although the rate of template hydrolysis is slightly reduced. The exception to this are mutants p66^{G231A}/p51 and p66^{Y232A}/p51 RT, which are delayed in their endonuclease capacity (Figure 5B, panel i, lanes 4 and 5). However, with prolonged incubation, these mutants yield the expected 62-nt product predictive of hydrolysis at template nucleotide −8 (Figure 5B, panel ii, lanes 4 and 5). In Figure 5C, the RT:RNA−DNA hybrid ratio was increased 2-fold, resulting in efficient −17 cleavage by p66^{G231A}/p51 but little difference with enzyme substituted at Tyr^{232} (Figure 5C, panel i, lanes 4 and 5, respectively); however, prolonged incubation again revealed efficient −8 cleavage by p66^{Y232A}/p51 RT (Figure 5C, panel ii, lane 5). The combined data of Figure 5 thus suggest altering Tyr^{232} of the primer grip may influence placement of an RNA−DNA hybrid within the C-terminal RNase H domain.

RNase H Activity of p66^{Y232A}/p51 RT Does Not Proceed through a −17 Intermediate. In order to better understand the altered RNase H activity of mutant p66^{Y232A}/p51 RT, a time course was performed at different enzyme−substrate ratios. Following high-voltage electrophoresis, hydrolysis products were visualized by either autoradiography (1:1 ratio of RT:RNA−DNA hybrid, Figure 6A,B) or phosphorimaging (2:1 ratio of RT:RNA−DNA hybrid, Figure 6C,D), the latter of which permitted a quantitative evaluation. By employing a low enzyme−substrate ratio and rapidly sampling reaction products, the profiles of Figure 6 revealed an unusual phenotype for p66^{Y232A}/p51 RT.

The hydrolysis profile of Figure 6A illustrates wild-type RT does not randomly cleave the RNA of an RNA−DNA hybrid but in the manner predicted by Peliska and Benkovic (1992); i.e., accumulation of the −17 cleavage intermediate is followed by processing as far as position −8. Figure 6C provides a quantitative evaluation of the same events, differing in that the enzyme−substrate ratio was increased 2-fold to ensure complete template hydrolysis. A plateau of −17 intermediate is evident over the initial 60 s, while the amount of 90-nt starting material continues to drop. As the initial substrate is exhausted, the −17 hydrolysis intermediate is processed and reflected by a rapid rise in −8 (62-nt) product. Under these conditions, the distribution of intermediates when hydrolysis is catalyzed by p66^{Y232A}/p51 RT (Figure 6B) is different. The 71-nt, −17 cleavage product is barely detected over the entire time course, while at the same time the −8 product steadily accumulates. In the phosphorimaging analysis of Figure 6D, 100% hydrolysis was achieved, ruling out the possibility that RNase H activity of p66^{Y232A}/p51 RT was qualitatively similar but slower than wild-type enzyme. One explanation for the RNase H phenotype of mutant p66^{Y232A}/p51 could be an enzyme devoid of RNase H activity but contaminated with the highly active bacterial counterpart. This possibility was eliminated by substituting Mg^{2+} with Mn^{2+}, since the *Escherichia coli* enzyme is virtually inactive in the presence of Mn^{2+} (Cirino et al., 1995). Under these conditions, the equivalent RNase H hydrolysis profile was observed for p66^{Y232A}/p51 RT (data not shown). In previous studies (Ghosh et al., 1995; Cirino et al., 1995) we could modulate RNase H function to direct cleavage exclusively to template nucleotide −17; the data of Figure 6 are the first report of an RNase H mutant whose hydrolytic action is directed to template nucleotide −8.

The data of Figure 6 might imply that altering Tyr^{232} of the primer grip loosens association of the p66 thumb

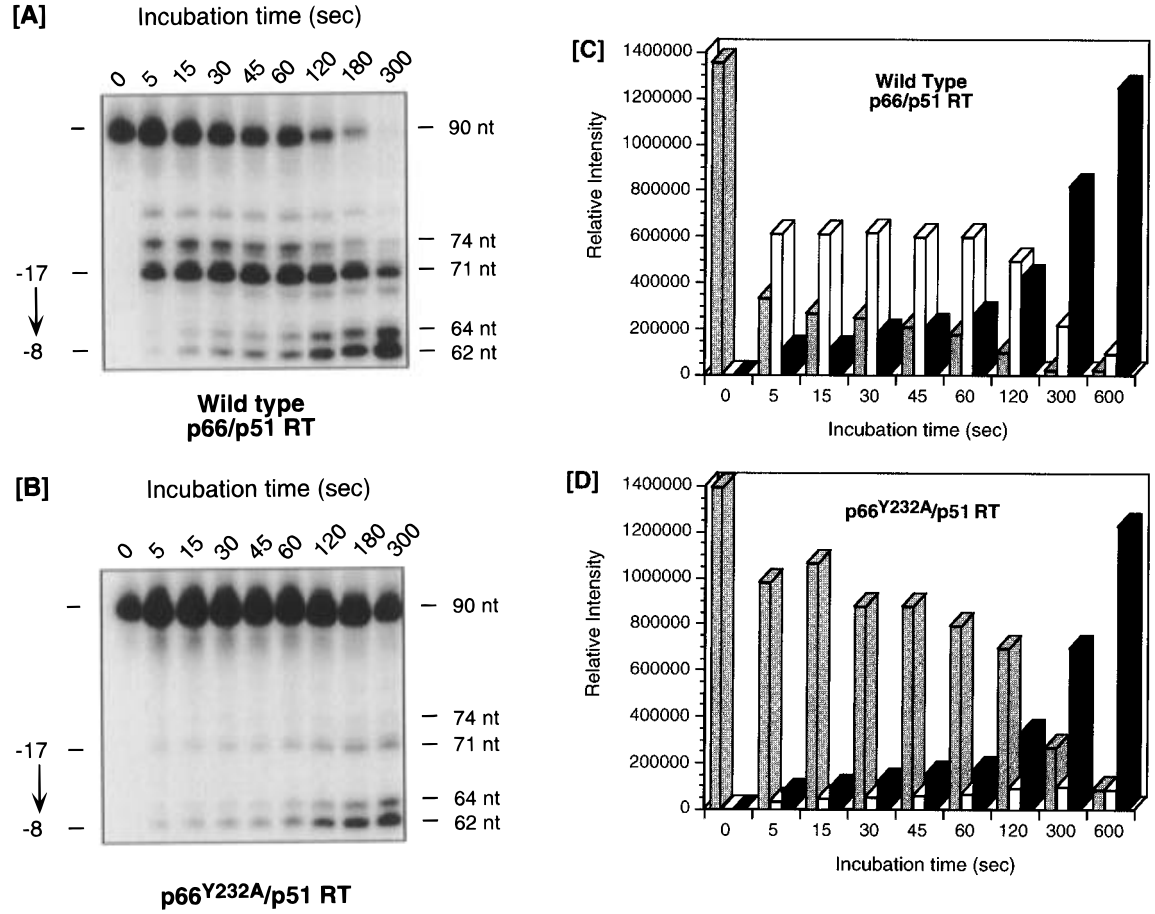

FIGURE 6: RNase H hydrolysis profiles of wild-type RT and mutant p66^{Y232A}/p51. [A] and [B] Autoradiographic analysis. RNase H activity was determined in the absence of DNA synthesis. In this experiment, enzyme and template-primer were incubated at a 1:1 stoichiometry. Samples were withdrawn for analysis between 5 and 300 s after hydrolysis was initiated. Nucleotide lengths were determined from DNA sequencing reactions run in parallel. [C] and [D] Phosphorimaging analysis. Experimental conditions differed from the data of [A] and [B] in that enzyme was added in a 2-fold excess over template-primer and the incubation period was increased to 10 min to ensure complete template hydrolysis by mutant enzyme. The intact 90-nt RNA template is represented by gray bars, while the −17 (71 nt) and −8 hydrolysis products (62 nt) are represented by white and black bars, respectively. Intensities of the hydrolysis products are in arbitrary units.

subdomain (Figure 1B) with the nucleic acid duplex, allowing it to move toward the RNase H catalytic center. Alternatively, mutant enzyme may have reduced affinity for template-primer but once bound would remain tightly associated with the nicked −17 hydrolysis intermediate and rapidly process to position −8. A two-step hydrolysis experiment was designed to distinguish between these possibilities and is presented in the following section.

Hydrolysis of a "Nicked" Substrate Representing a −17 Cleavage Intermediate. Although the ability of p66^{Y232A}/p51 RT to cleave our model RNA−DNA hybrid at position −17 was reduced, we were interested in whether the mutant might better recognize and hydrolyze a "relaxed" substrate which had been cleaved at this position. This possibility was investigated by exploiting the properties of a unique HIV-1 RNase H mutant prepared in our laboratory and a "two-step" hydrolysis experiment. The selectively deleted mutant p66Δ8/p51, containing an eight-residue truncation in α-helix E′ of its RNase H domain, is fully competent as an endoribonuclease but impaired in its directional processing function (Ghosh et al., 1995). The rationale for our two-step experiment is outlined in Figure 7A. Preincubation of the RNA−DNA hybrid with p66Δ8/p51 RT for 30 min at 37 °C generates a nucleic acid duplex whose template is cleaved predominantly at position −17. In a second step, the nicked duplex is incubated with wild-type or mutant RT, after which their RNase H hydrolysis profiles are followed for an additional 10 min. As control, the RNase H profile of mutant p66Δ8/p51 alone was determined over a total incubation time of 40 min (Figure 7B). A similar approach was adopted by Wöhrl et al. (1994) to complement a processivity defect of p51 EIAV RT by the p66 EIAV subunit and by Amacker et al. (1995) to study the p51 and p66 subunits comprising feline immunodeficiency virus RT.

The results of our analysis are presented in Figure 7C−F. The precleaved substrate appears to offer no selective advantage to mutant p66^{Y232A}/p51 which, if anything, is slightly less active (Figure 7E,F). In contrast, wild-type enzyme recognizes and hydrolyzes the nicked substrate with almost the same efficiency as the intact RNA−DNA hybrid (Figure 7C,D). To address the possibility of different affinities of p66Δ8/p51 and p66^{Y232A}/p51 RT for the RNA−DNA hybrid, the experiment of Figure 7 was repeated and the primer grip mutant was added in a 4-fold excess over p66Δ8/p51. Under these conditions, the rate at which the −17 nicked intermediate was hydrolyzed to position −8 was unaffected (data not shown). The combined data of Figures 5−7 may indicate that the inability of RT mutated at Tyr^{232} to process an RNA−DNA hybrid from position −17 reflects transient occupancy of the RNase H active center by this

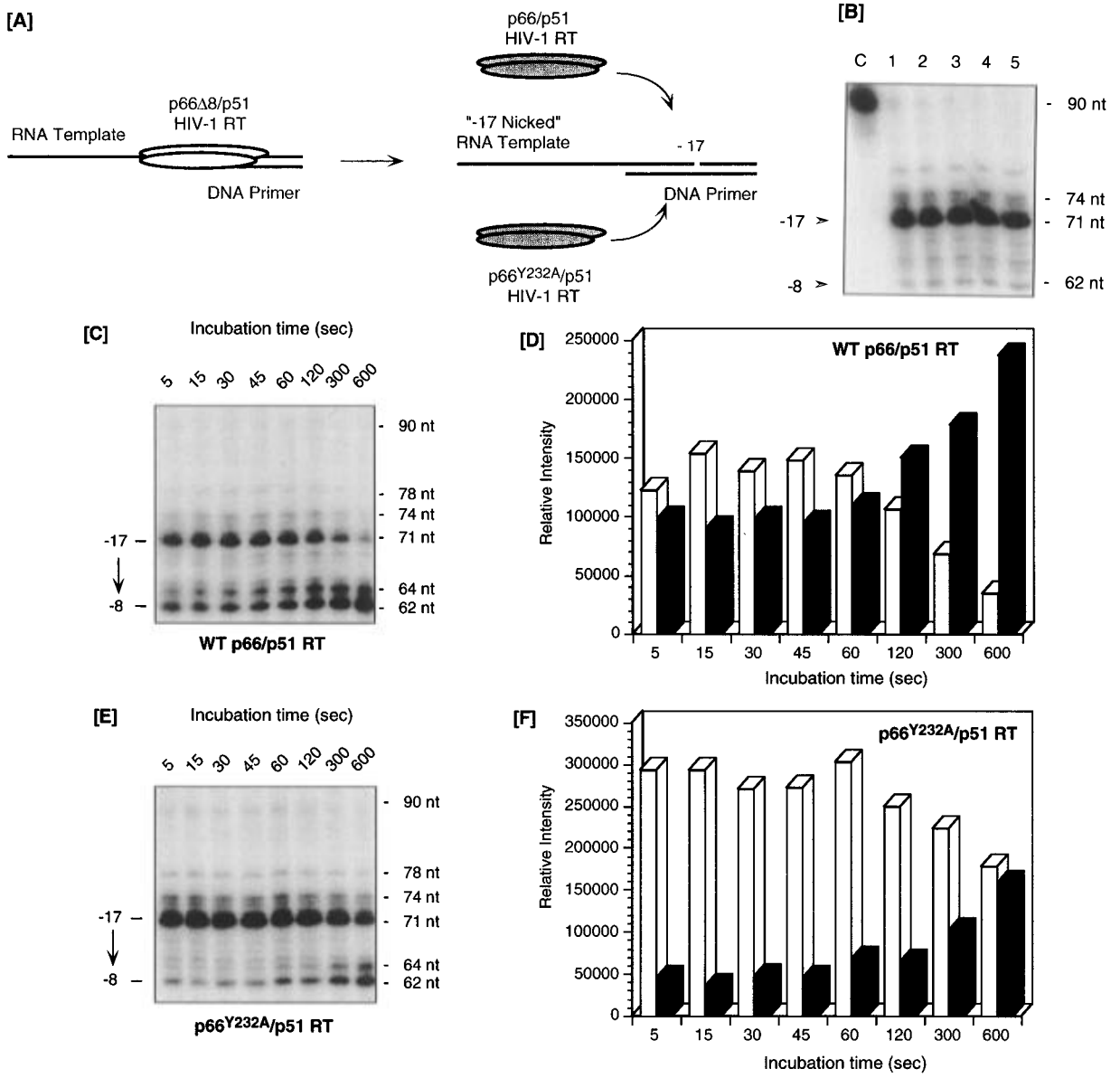

FIGURE 7: Hydrolysis of a precleaved (−17) substrate by wild-type RT and mutant p66^{Y232A}/p51. [A] Schematic representation of the two-step hydrolysis reaction. In a first reaction, template-primer is incubated for 30 min with RT mutant p66Δ8/p51. Due to truncation of α-helix E′ of the RNase H domain, this mutant cleaves the substrate at position −17 but fails to proceed further (Ghosh et al., 1995). This procedure thus generates a −17 hydrolysis intermediate. In a subsequent step, this mixture is supplemented with wild-type RT or mutant p66^{Y232A}/p51, and their ability to cleave the −17 intermediate is evaluated. [B] Preparation of the "nicked" −17 hydrolysis intermediate by RT mutant p66Δ8/p51. C, uncleaved template. Lanes 1−5, −17 hydrolysis product following incubation with p66Δ8/p51 RT for 30, 32.5, 35, 37.5, and 40 min, respectively. [C] and [E] Autoradiographic analysis of the activity of wild-type ([C]) and mutant enzyme ([E]) on the precleaved substrate. Note the absence in both cases of the 90-nt template at the outset of the time course, indicating 100% endonucleolytic precleavage with p66Δ8/p51 RT. [D] and [F] Quantitative phosphorimaging analysis of the data of panels [C] and [E], respectively. White and black bars represent the −17 and −8 hydrolysis products, respectively.

region of template-primer. Conceivably, the RNA−DNA hybrid is released from the DNA polymerase catalytic center as a consequence of a structurally compromised primer grip, relocating template nucleotide −8 sufficiently close to the RNase H active center to permit hydrolysis.

Infectivity of Recombinant Virus Carrying Primer Grip Mutations. In an attempt to correlate *in* vitro alterations to HIV-1 RT with altered viral replication, recombinant virus was constructed containing mutations between Trp^{229} and His^{235}. In contrast to our *in vitro* approach of subunit-selective mutagenesis, primer grip mutations are present in both p66 and p51 RT following maturation of the *gag−pol* precursor polyprotein. Although substituting Leu^{234} with Ala induced a dimerization defect and precluded further *in* vitro analysis of this mutant, we were interested in determining whether the *in vivo* consequences were as severe. The results for each primer grip mutation have been summarized in Table 1.

As previously reported (Jacques et al., 1994a), substituting Trp^{229} with Ala resulted in the production of noninfectious virions, although contained correctly processed p66/p51 RT and CA p24 could be detected following transfection. A similar observation was made when Met^{230} and Leu^{234} were substituted with Ala. Although a severe defect to RT-associated activities was evident for mutant p66^{Y232A}/p51, it was possible to recover infectious virus, albeit at 0.1% of the level determined for wild-type virus. Although confirmatory data are unavailable, this may suggest that, in the

Table 1: Infectivity of Recombinant HIV-1 Containing Mutations between Trp^{229} and His^{235} of Its RT Gene[a]

primer grip mutation	infectivity (iu/mL)	CA p24 (WB)	RT p66/p51 (WB)
p66/p51 WT	100 000	+	+
$p66^{W229A}/p51^{W229A}$		+	+
$p66^{M230A}/p51^{M230A}$		+	+
$p66^{G231A}/p51^{G231A}$	100 000	+	+
$p66^{Y232A}/p51^{Y232A}$	100	+	+
$p66^{E233A}/p51^{E233A}$	100 000	+	+
$p66^{L234A}/p51^{L234A}$		±	+
$p66^{H235A}/p51^{H235A}$	100 000	+	+

[a] In contrast to *in vitro* studies, recombinant virus contains mutations in both RT subunits. Infectivity is determined in infectious units (iu)/mL. The presence of p24 capsid protein (CA p24) and p66/p51 RT in virions was determined immunologically via western blotting (WB) with the appropriate polyclonal antibodies.

context of additional virion components (e.g., nucleocapsid), defects to Tyr^{232} of the primer grip can be tolerated. Finally, the infectivity of virions containing Ala substitutions at positions Gly^{231}, Glu^{233}, and His^{235} was indistinguishable from wild-type virus, which correlates well with the *in vitro* analyses of Figures 3−5.

DISCUSSION

The cocrystal of p66/p51 HIV-1 RT with double-stranded DNA (Jacobo-Molina et al., 1993) implicates the $\beta12-\beta13$ hairpin of its p66 subunit ($Phe^{227}-His^{235}$) in orienting the primer terminus for nucleophilic attack on an incoming dNTP. To experimentally assess whether the entire motif or a subset of residues mediates this function, subunit-selective mutagenesis and *in vitro* reconstitution (Le Grice et al., 1991) were exploited to evaluate the consequences of altering p66 residues $Met^{230}-His^{235}$. Alanine scanning was chosen as a first step in our structure−function analysis, since it minimizes unfavorable steric contacts and avoids imposing new charge interactions or hydrogen bonds (Carter & Wells, 1988). For the HIV-1 enzyme, the same approach was recently applied to a systematic study of a motif within the p66 thumb subdomain (Beard et al., 1994; Bebenek et al., 1995). Data presented here indicate that substituting amino acids of the $\beta12-\beta13$ loop (Met^{230} and Gly^{231}) and immediately flanking residues (Trp^{229} and Tyr^{232}) has consequences for the DNA polymerase catalytic center which also manifest themselves in the catalytic properties of the C-terminal RNase H domain.

The -Trp^{229}-Met^{230}-Gly^{231}-Tyr^{232}- quartet appears the most critical feature of the primer grip. A comparative analysis of several retroviral sequences (Xiong & Eichbusch, 1990) suggests a preference for aromatic residues at positions 229 and 232. Roles for these residues in (a) interacting with and positioning template-primer or (b) providing the appropriate architecture of the primer grip might be considered. The former role implies that the π-electron-rich side chains of Trp^{229} and Tyr^{232} participate in stacking interactions with nucleic acid bases (essentially as the outermost "prongs" of a fork), precedent for which is provided by the 7-methylguanosine 5′-monophosphate−tryptamine cocrystal (Kamiichi et al., 1986) and the HIV-1 nucleocapsid protein (Lam et al., 1994). Alternatively, an interaction between side chains of these residues may be required to stabilize the $\beta12-\beta13$ connecting loop, which constitutes a tight β-turn. The structural models of Figure 1 tend to support the latter notion. Crystallographic data from unliganded HIV-1 RT (Rodgers et al., 1995) indicate the side chains of Trp^{229}, Met^{230}, and Tyr^{232} do not point outward toward nucleic acid but rather are inserted into the core region between β-strands 12 and 13 and the DNA polymerase active site. Together with additional hydrophobic interactions (possibly including the side chains of Leu^{234} and Phe^{227}) these side chains appear to stabilize β-strands 12 and 13. The geometry on the $\beta12-\beta13$ connecting loop, together with a strong preference in retroviral RT for Gly at this position (Xiong & Eichbusch, 1990), predicts the $Gly^{231} \rightarrow Ala^{231}$ replacement would be detrimental to primer grip architecture. Although heparin challenge experiments (data not shown) indicate the affinity of $p66^{G231A}$/p51 RT for template-primer is reduced, this mutant displays considerable activity, as evidenced by the DNA synthesis profiles of Figures 3 and 4. Hydrophobic interactions involving the side chains of Trp^{229}, Met^{230}, and Tyr^{232} may therefore be sufficient to overcome the energetic cost of placing Ala^{231} in an unfavorable conformation. In contrast, altering any other residue of the quartet appears to significantly perturb this hydrophobic core and destabilize the primer grip.

Interdependence of the N-terminal DNA polymerase and C-terminal RNase H catalytic centers of HIV-1 RT also provided an opportunity of evaluating how altered contact to the primer grip of $p66^{Y232A}$/p51 RT influences how the RNA moiety of an RNA−DNA hybrid is positioned in the RNase H domain. One possibility might be that the altered RNase H hydrolysis profile obtained with $p66^{Y232A}$/p51 RT reflects alternative positioning of template-primer within the nucleic acid binding cleft. In this model, the hybrid would be sequestered by RT in two distinct conformations. When nucleic acid is correctly and stably positioned at the DNA polymerase catalytic center, cleavage at template nucleotide −17 is favored, followed by processing as far as position −8, as demonstrated by Peliska and Benkovic (1992). With mutant $p66^{Y232A}$/p51, this complex may be nonproductive with respect to RNase H activity, resulting in dissociation of the nucleoprotein complex without hydrolysis at position −17. However, mutant RT may be capable of binding the RNA−DNA hybrid in an alternative conformation which is competent for hydrolysis at template nucleotide −8.

As illustrated in Figure 1B, β-strands 12−15 of p66 RT constitute a sheet at the base of its thumb subdomain. Altering Tyr^{232} of β-strand 13 may compromise the architecture of this sheet to inhibit a proposed role for its thumb and palm in positioning template-primer and translocation (Jacobo-Molina et al., 1993; Nanni et al., 1993). The RNase H phenotype of $p66^{Y232A}$/p51 RT might then reflect movement of the RNA−DNA duplex in the nucleic acid binding cleft while contact to the single-stranded template is maintained through the "template grip" (Jacobo-Molina et al., 1993; Nanni et al., 1993). Under these conditions, the replication complex described by Wöhrl et al. (1995a) suggests template nucleotide −8 might be sufficiently close to the RNase H catalytic center to allow hydrolysis, perhaps facilitated by distorted geometry of the nucleic acid duplex between positions −7 and −11 (Jacobo-Molina et al., 1993; Metzger et al., 1993).

In the absence of a crystal structure for $p66^{Y232A}$/p51 RT, these models remain speculative. However, data from this report illustrate the importance of further dissecting the primer grip and how this structure impinges upon the DNA

polymerase and RNase H catalytic centers. As efforts in this direction proceed, they may open the possibility of developing therapeutic agents act by altering subdomain and/or subunit geometry to impair the interaction with nucleic acid rather than polymerization events. Alternatively, preliminary data with enzyme substituted at Leu^{234} suggest the concept of peptide-based inhibitors of dimerization (Divita et al., 1994) may also be applicable to the primer grip.

REFERENCES

Adachi, A., Gendelman, H. R., Koenig, S., Folks, T., Willey, R., Rabson, A., & Martin, M. A. (1986) *J. Virol. 59*, 284−291.

Amacker, M., Hottiger, M., & Hubscher, U. (1995) *J. Virol. 69*, 6273−6279.

Arts, E. J., Ghosh, M., Jacques, P. S., Ehresmann, B., & Le Grice, S. F. J. (1996) *J. Biol. Chem. 271*, 9054−9061.

Beard, W. A., Stahl, S. J., Kim, H.-R., Bebenek, K., Kumar, A., Strub, M.-P., Becerra, S. P., Kunkel, T. A., & Wilson, S. H. (1994) *J. Biol. Chem. 269*, 28091−28097.

Bebenek, K., Beard, W. A., Casas-Finet, J. R., Kim, H.-R., Darden, T. A., Wilson, S. H., & Kunkel, T. A. (1995) *J. Biol. Chem. 270*, 19518−19523.

Carter, P., & Wells, J. A. (1988) *Nature (London) 232*, 564−568.

Chen, C., & Okayama, H. (1987) *Mol. Cell. Biol. 7*, 2745−2752.

Cirino, N. M., Cameron, C. E., Smith, J. S., Rausch, J. S., Roth, M. J., Benkovic, S. J., & Le Grice, S. F. J. (1995) *Biochemistry 34*, 9936−9943.

Divita, G., Müller, B., Immendörfer, U., Gautel, M., Rittinger, K., Restle, T., & Goody, R. S. (1993) *Biochemistry 32*, 7966−7971.

Divita, G., Restle, T., Goody, R. S., Cherrman, J.-C., & Ballion, J. G. (1994) *J. Biol. Chem. 269*, 13080−13083.

Ghosh, M., Howard, K. J., Cameron, C. E., Hughes, S. H., Benkovic, S. J., & Le Grice, S. F. J. (1995) *J. Biol. Chem. 270*, 7068−7076.

Goff, S. P., Trakiman, P., & Baltimore, D. (1981) *J. Virol. 38*, 239−248.

Hochuli, E., Bannwarth, W., Döbeli, H., Gentz, R., & Stüber, D. (1988) *Bio/Technology 6*, 1321−1325.

Jacobo-Molina, A., Ding, J., Nanni, R. G., Clark, A. D., Jr., Lu, X., Tantillo, C., Williams, R. L., Kamer, G., Ferris, A. L., Clark, P., Hizi, A., Hughes, S. H., & Arnold, E. (1993) *Proc. Natl. Acad. Sci. U.S.A. 90*, 6320−6324.

Jacques, P. S., Wöhrl, B. M., Ottmann, M., Darlix, J. L., & Le Grice, S. F. J. (1994a) *J. Biol. Chem. 269*, 26472−26478.

Jacques, P. S., Wöhrl, B. M., Howard, K. J., & Le Grice, S. F. J. (1994b) *J. Biol. Chem. 269*, 1388−1393.

Jonckheere, H., Taymans, J. M., Balzarini, J., Velazquez, S., Camarasa, M.-J., Desmyter, J., De Clerq, E., & Anne, J. (1994) *J. Biol. Chem. 269*, 26255−26258.

Kamiichi, K., Danshita, M., Minamino, N., Doi, M., Ishida, T., & Inoue, M. (1986) *FEBS Lett. 195*, 57−60.

Kohlstaedt, L. A., Wang, J., Friedman, M., Rice, P. A., & Steitz, T. A. (1992) *Science 256*, 1783−1790.

Lam, W.-C., Maki, A., Casa-Finet, J. R., Erickson, J. W., Kane, B. P., Sowder, R. C., II, & Henderson, L. E. (1994) *Biochemistry 33*, 10693−10700.

Le Grice, S. F. J. (1995) *Protein Pept. Lett. 2*, 381−390.

Le Grice, S. F. J., & Grüninger-Leitch, F. (1990) *Eur. J. Biochem. 187*, 307−314.

Le Grice, S. F. J., Naas, T., Wohlgensinger, B., & Schatz, O. (1991) *EMBO J. 10*, 3905−3911.

Le Grice, S. F. J., Cameron, C. E., & Benkovic, S. J. (1995) *Methods Enzymol. 262*, 130−147.

Metzger, W., Hermann, T., Schatz, O., Le Grice, S. F. J., & Heumann, H. (1993) *Proc. Natl. Acad. Sci. U.S.A. 90*, 5909−5913.

Müller, B., Restle, T., Reinstein, J., & Goody, R. S. (1991) *Biochemistry 30*, 3709−3715.

Nanni, R. G., Ding, J., Jacobo-Molina, A., Hughes, S. H., & Arnold, E. A. (1993) *Perspect. Drug Dis. Design 1*, 129−150.

Peliska, J. A., & Benkovic, S. J. (1992) *Science 258*, 1112−1118.

Rodgers, D. W., Gamblin, S. J., Harris, B. A., Ray, S., Culp, J. S., Hellmig, B., Woolf, D. J., Debouck, C., & Harrison, S. C. (1995) *Proc. Natl. Acad. Sci. U.S.A. 92*, 1222−1226.

Schatz, O., Cromme, F., Gruninger-Leitch, F., & Le Grice, S. F. J. (1989) *FEBS Lett. 257*, 311−314.

Smerdon, S. J., Jäger, J., Wang, J., Kohlstaedt, L. A., Chirino, A. J., Friedman, M., Rice, P. A., & Steitz, T. A. (1994) *Proc. Natl. Acad. Sci. U.S.A. 91*, 3911−3915.

Smith, S. D., Shatsky, M., Cohen, P. S., Warnke, R., Link, M. P., & Glader, B. E. (1984) *Cancer Res. 44*, 5657−5660.

Wöhrl, B. M., Howard, K. J., Jacques, P. S., & Le Grice, S. F. J. (1994) *J. Biol. Chem. 269*, 8541−8548.

Wöhrl, B. M., Tantillo, C., Arnold, E., & Le Grice, S. F. J. (1995a) *Biochemistry 34*, 5343−5350.

Wöhrl, B. M., Georgiadis, M. M., Telesnitsky, A., Hendrickson, W. A., & Le Grice, S. F. J. (1995b) *Science 267*, 96−99.

Xiong, Y., & Eickbush, T. H. (1990) *EMBO J. 9*, 3353−3362.

BI952773J